69th Meeting of the AEROBALLISTIC RANGE ASSOCIATION
Bath, England, UK, October 7 – 12, 2018.

Recent Upgrades for the NASA Ames Vertical Gun Range

Charles J. Cornelison[1]
NASA-Ames Research Center, Moffett Field, CA 94035

Jon-Pierre Wiens[2], Alfredo J. Perez[3]
Aerodyne Industries, Moffett Field, CA 94035

ABSTRACT

Recent upgrades to the performance capabilities of the NASA Ames Vertical Gun Range (AVGR) are presented. Upgrades include: the successful implementation of a fast-acting, gun-gases suppression valve to minimize target contamination and perturbations to both the target and ejecta; powder gun and light-gas gun operational parameter adjustments to provide clean, low-speed test conditions; a liquid nitrogen-based system and methodology for chilling targets and/or other impact chamber situated equipment; and imaging system capabilities enhancements to enable observing 50 μm particles traveling at 2 km/s. Many of these performance improvements were motivated by AVGR customer requirements for very clean shot conditions at speeds below 1.9 km/s and to provide testing in support of proposed NASA missions to Enceladus and 16-Psyche.

I. INTRODUCTION

The Ames Vertical Gun Range (AVGR) is NASA's premier facility for performing hypervelocity impact testing as it pertains to Planetary Geology and Geophysics (PG&G) applications. The facility became operational in 1966 in support of the Apollo program as a means to develop a better understanding of lunar surface geomorphological characteristics. Data obtained from these early tests was instrumental in helping design the Lunar Excursion Module (LEM) and assessing potential landing sites. At the successful conclusion of the Apollo program, it was recognized that the AVGR was an extremely useful tool for investigating the physics and phenomena underlying crater formation and debris dispersion processes, not only for the moon, but for all terrestrial planets, moons, asteroids, comets, etc. in the solar system. As such, the AVGR has been and continues to be a workhorse for the PG&G community [10].

In addition, the AVGR has generated critical data in support of several major, NASA programs in the arenas of mission enabling technology development and vehicle survivability/vulnerability. Examples include: Aerogel-based particle capture medium development for Stardust; Mission

[1] Facility Manager, Ballistic Range Complex, Thermo-Physics Facilities Branch.
[2] Imaging Technologist, Ballistic Range Complex, Thermo-Physics Facilities Branch
[3] Electronics Engineering Technician, Ballistic Range Complex, Thermo-Physics Facilities Branch

concept development, instrumentation selection/specification, and post-encounter data analysis for Deep Impact; Component vulnerability and vehicle survivability for Cassini, Mars Odyssey, and Mars Exploration Rovers (MER). In addition, asteroid defense studies focused on hypervelocity momentum transfer and target disruption continue to be an ongoing focus at the AVGR.

What makes the AVGR truly unique, is a combination of its hinged gun beam and large impact/vacuum chamber. Constructed, in part, from a 1950's era Nike missile launching platform, the gun beam can be oriented such that the bore axis of the projectile launching gun (either .30 cal. light-gas or powder) can be varied from horizontal to vertical in 15° increments (see figure 1). This enables varying the impact angle relative to the gravity vector, a capability that is particularly useful and necessary when impacting targets such as regolith analogs, sand, gravel, water, etc. [3] In addition, the large impact chamber (see figure 2) can be evacuated (to pressures less than 0.5 Torr) to simulate impacts on celestial bodies with little, or no, atmosphere, or backfilled with a variety of test gases to simulate impacts on planets and moons with atmospheres. Both features are essential when simulating and studying crater formation and ejecta dispersion processes.

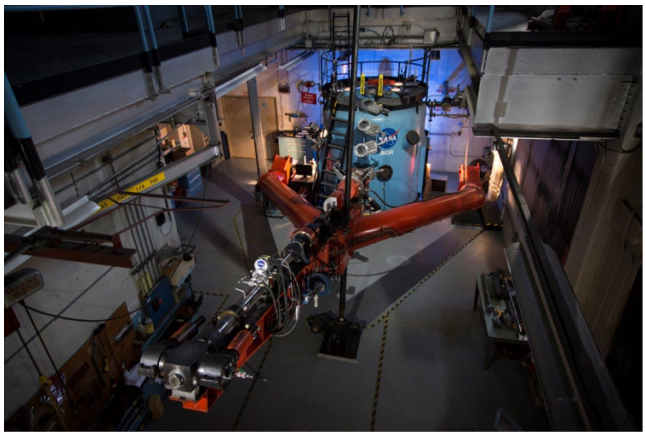

Figure 1: AVGR gun beam and impact chamber, 15-degree orientation.

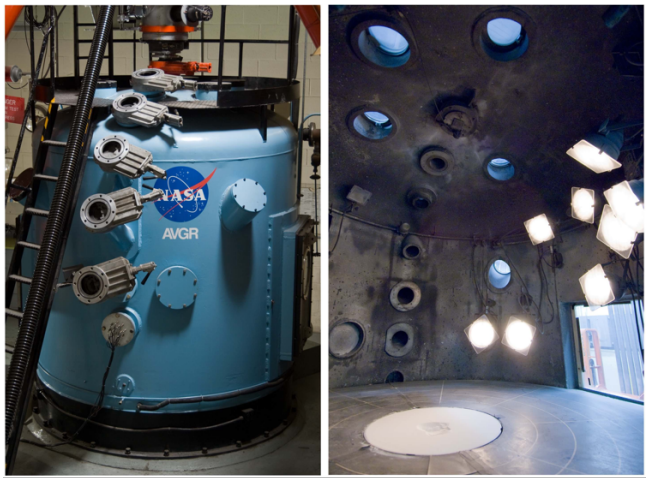

Figure 2: AVGR impact/vacuum chamber (exterior and interior views).

A .30 cal. powder gun and light-gas gun are used to launch spherical particles ranging in size from 1/16" to 1/4" (1.6 to 6.4 mm) diameter to velocities ranging from 0.5 to 7.0 km/s. Typical particle materials include: metals (aluminum, copper, brass, steel), glass (quartz, borosilicate-Pyrex®, soda-lime), plastics (nylon, polyethylene, PMMA) and mineral (basalt, agate, dolomite). In addition, cylinders of a similar diameter range and with an L/D of 2 or less, plus clusters (analogous to a shotgun blast) of micro-particles (3-100 μm in diameter) can be launched as well.

Much of the data obtained from typical AVGR experiments, in addition to actual cratered targets, are the high-speed video recordings of the impact event. The current imaging system consists of pairs of Vision Research Phantom V10, V12.1 and V2512

Figure 3: PIV (Particle Image Velocimetry) experiment preparation.

color cameras, plus a pair of Shimadzu HPV-1 monochrome cameras. This suite of cameras combined with various lenses, lighting and viewing port locations allow a wide variety of perspectives, frame rates, resolution levels (see Table 1, from Ref. 11), etc. In addition, spectroscopic and PIV (particle image velocimetry) instrumentation (see figure 3) can be implemented by way of special arrangement.

Table 1: Resolution (Horizon and Vertical) vs Frames Per Second (FPS) for Phantom V10, V12.1 and V2512 cameras [11].

V10 Resolution		
H	V	Max FPS
2400	1800	480
1600	1200	1016
1920	1080	978
1440	1440	943
1280	720	1992
1152	1152	1419
960	720	2619
960	480	3902
768	768	2919
576	576	4756
576	288	9280
480	480	6420
192	192	24242
96	96	51282
96	8	153846

V12 Resolution		
H	V	Max FPS
1280	800	6242
1280	720	6933
1024	768	7921
1024	512	11854
800	600	11364
720	576	13485
640	480	18769
512	512	20978
512	384	27865
320	240	64516
256	256	66997
256	128	128998
128	64	330469
128	32	560224
128	16	852514

V2512 Resolution		
H	V	Max FPS
1280	800	25600
1280	720	28500
1024	800	30500
1024	512	47300
896	800	33600
768	768	39100
640	480	69900
512	512	75400
512	384	99500
384	256	170600
256	256	205000
256	128	375700
128	64	764700
128	32	1000000
128	16	1000000

II. GUN GASES SUPPRESSION VALVE

One of the challenges that is common to both light-gas gun and powder gun testing is minimizing the amount of target contamination and perturbations to both the target and ejecta due to the impingement of trailing gun gases. In the AVGR, this problem is partially mitigated by the relatively large impact chamber volume (approx. 500 ft^3 or 14 m^3). Targets are positioned nearly 20 ft. (6 m) away from the gun muzzle and the gun gases are able to expand into the impact chamber with only a slight pressure increase which, in turn, greatly dissipates any resultant pressure pulses imparted to the target. However, for low density target materials such as pumice and dolomite, this is not sufficient and the gun gases can affect both the crater shape and ejecta dispersion patterns. To remedy this situation, a fast acting, solenoid actuated, spring-operated flapper valve, affectionately referred to as the "rat trap," was developed. This valve is a portable device that can be mounted at any of the impact chamber ports (see figure 4). In addition, each port is equipped with a vent flange that is configured in such a manner so that when the valve closes, just after the

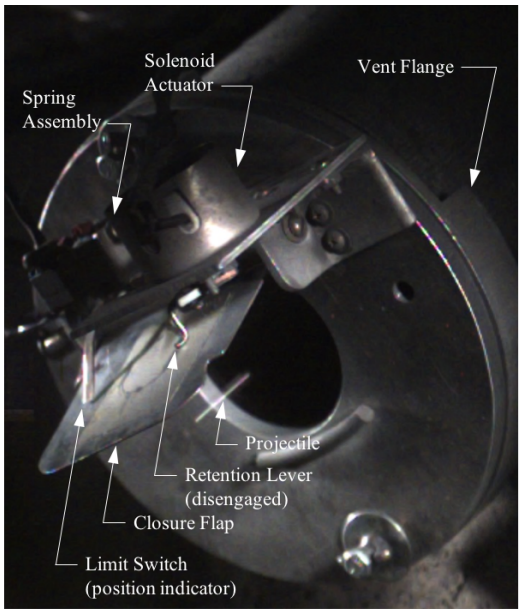

Figure 4: Gun gases suppression valve, aka the "Rat Trap" mounted on the Impact Chamber 45º port.

impactor/projectile passes, the trailing gun gases are vented out along the chamber walls, away from the target.

The valve can be triggered off of various timing events that occur during the gun firing sequence so that the valve closes several to 10 milliseconds after the impactor passes and well before the gun gases arrive for most test conditions. In short, a trigger pulse initiates a 30 VDC capacitor discharge which, in turn, activates a solenoid that disengages the retention lever. The torsional spring then closes the valve, redirecting the gun gases out the vent flange ports. The time from trigger pulse to valve closure is on the order of 30 msec. Figure 5 shows identical test conditions, with and without the rat trap. Clearly, use of the rat trap minimizes target contamination and perturbations to both the target and ejecta dispersion.

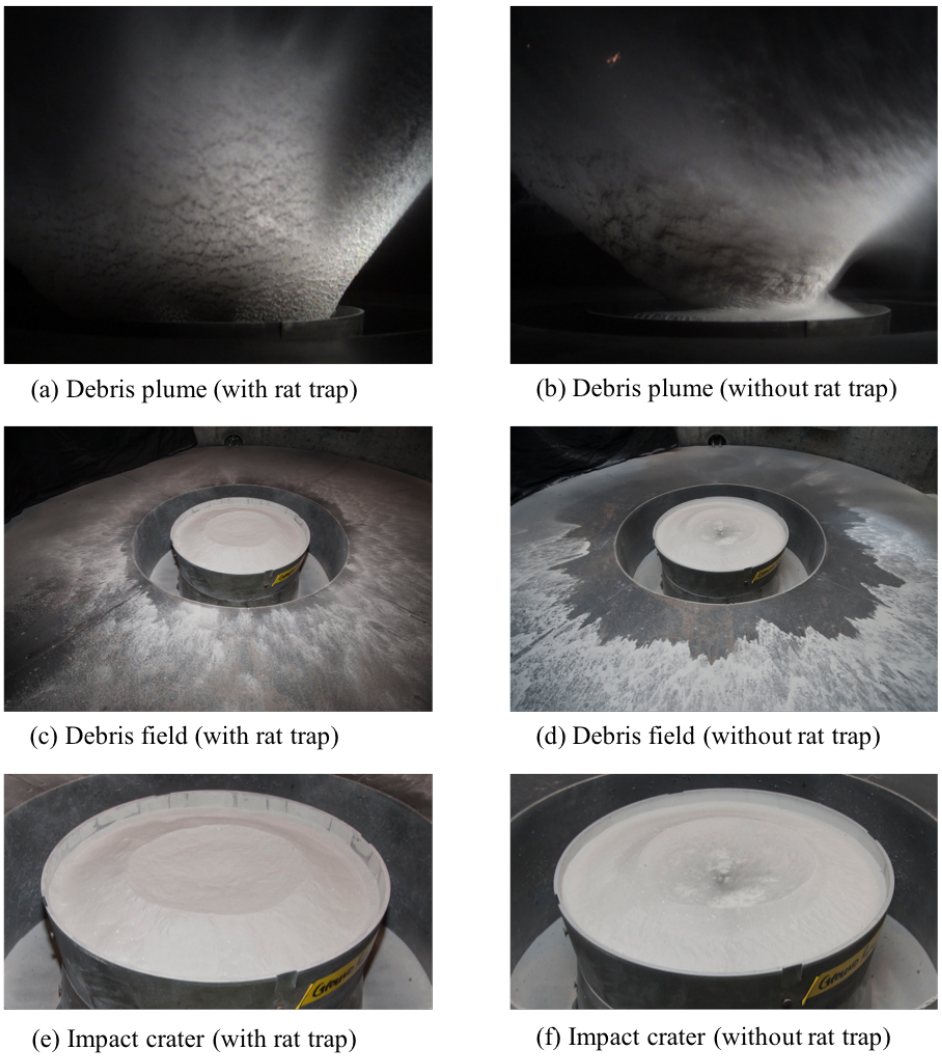

(a) Debris plume (with rat trap)

(b) Debris plume (without rat trap)

(c) Debris field (with rat trap)

(d) Debris field (without rat trap)

(e) Impact crater (with rat trap)

(f) Impact crater (without rat trap)

Figure 5: Results of identical tests – ¼" (6.4 mm) dia. Aluminum sphere at 5 km/s, 45° into pumice, with and without the gun gases suppression valve (rat trap).

Although the gun gases suppression valve is extremely effective in providing clean impacts for light-gas gun testing, it isn't as efficacious for powder gun operations below 1.9 km/s. For these conditions, the impactor is often closely followed by unburnt or partially burnt gun powder grains

and the situation worsens as the velocity decreases. For single particle (1/16" to 1/4" or 1.6 to 6.4 mm diameter) impacts this is typically inconsequential in that the impactor mass is much larger (2 to 3 orders of magnitude) than the accompanying gun powder particulates. However, for micro-particle impacts, wherein the impactors are of comparable size (10's of microns in diameter), this can be problematic.

What is believed to be the cause of this behavior is as follows. To begin with, the AVGR powder gun utilizes a standard, .300 caliber, Weatherby Magnum casing (see figure 6a) that is hand loaded with a specific gun powder charge to produce a desired impact velocity for a given launch mass. Typical launch masses are much smaller (<5%) than the mass of a typical bullet fired with the same casing. As a result, an AVGR launch package accelerates much quicker and traverses the gun barrel much faster than a typical bullet fired with a .300 Weatherby rifle. Consequently, combustion pressure and temperature pulses don't get as high or last as long which, in turn, diminishes the reaction rates. In addition, since the casing volume is fixed, a powder charge for moderate to low speed only fills a small portion of the casing volume. For example, the powder charge for a typical 1 km/s condition fills only 20% of the casing. To exacerbate this situation, when the gun is oriented and loaded for vertical impact (shooting downward), the powder charge rests upon the sabot base, nearly 2" (5 cm) away from the primer.

(a) Standard Powder Gun Casing (b) Custom Powder Gun Casing

Figure 6: Sectional views of the AVGR .30 caliber Powder Gun casings – Standard .300 Weatherby Magnum and Custom (with only 25% internal volume).

As a result of these contributing factors, when the gun is fired not all of the powder has an opportunity to burn completely before the launch package (projectile and sabot) exits the gun barrel. Consequently, the remaining unburnt and/or partially burnt grains tend to travel in close proximity to the impactor (too close to be stopped by the rat trap) until they too hit the target, thus, tarnishing the impact test results.

To mitigate this problem, three approaches were explored: (A) using gun powders with different burning rates; (B) using a customized casing with reduced (25% of the original) internal volume (see figure 6b); and (C) operating the light-gas gun with both a slower burning powder and different pump tube gases (helium or argon) in lieu of hydrogen. The results of these studies are as follows.

A. Gun Powders

For many years, the traditional gun powder used for AVGR .30 cal. powder gun operations has been Alliant's "Unique" smokeless powder. For this comparative study, three Hodgdon powders (Universal, International and Clays), of differing burning rates, were used to see which powder provides the cleanest results for impact velocities at or below 1.9km/s. As can be seen in Table 2 [from Ref. 6], Hodgdon Universal has a similar burning rate as Unique. Whereas, International and Clays are progressively faster burning powders.

Table 2: Relative burning rates for commercially available smokeless powders [6].

Relative Burn Rates From Fastest To Slowest Provided by HODGDON

1	NORMA R1	51	Alliant Blue Dot	101	Hodgdon VARGET
2	VihtaVuori N310	52	Accurate Arms No. 7	102	IMR, Co IMR 4320
3	Accurate Arms Nitro 100	53	Alliant Pro Reach	103	Winchester 748
4	Alliant e3	54	Hodgdon LONGSHOT	104	Hodgdon BL-C(2)
5	Hodgdon TITEWAD	55	Alliant 410	105	Hodgdon CFE 223
6	Ramshot Competition	56	Alliant 2400	106	Hodgdon *LEVEREVOLUTION*
7	Alliant Red Dot	57	Ramshot Enforcer	107	Hodgdon H380
8	Alliant Promo	58	Accurate Arms No. 9	108	Ramshot Big Game
9	Hodgdon CLAYS	59	Accurate Arms 4100	109	VihtaVuori H540
10	IMR, Co IMR RED	60	Alliant Steel	110	Winchester 760
11	Alliant Clay Dot	61	NORMA R123	111	Hodgdon H414
12	Hodgdon Hi-Skor 700-X	62	VihtaVuori N110	112	VihtaVuori N150
13	Alliant Bullseye	63	Hodgdon LIL' GUN	113	Accurate Arms 2700
14	IMR, Co IMR TARGET	64	Hodgdon H110	114	IMR, Co IMR 4350
15	Hodgdon TITEGROUP	65	Winchester 296	115	IMR, Co IMR 4451
16	Alliant American Select	66	IMR, Co IMR 4227	116	Hodgdon H4350
17	Accurate Arms Solo 1000	67	Accurate Arms 5744	117	Alliant Reloder 17
18	Alliant Green Dot	68	Accurate Arms 1680	118	Accurate Arms 4350
19	IMR , Co IMR GREEN	69	Hodgdon CFE BLK	119	NORMA 204
20	Winchester WST	70	NORMA 200	120	Hodgdon HYBRID 100V
21	Hodgdon Trail Boss	71	Alliant Reloder 7	121	VihtaVuori N550
22	Winchester Super Handicap	72	IMR, Co IMR 4198	122	Alliant Reloder 19
23	Hodgdon INTERNATIONAL	73	Hodgdon H4198	123	IMR, Co IMR 4831
24	Accurate Arms Solo 1250	74	VihtaVuori N120	124	Ramshot Hunter
25	VihtaVuori N320	75	Hodgdon H322	125	Accurate Arms 3100
26	Accurate Arms No. 2	76	Accurate Arms 2015BR	126	VihtaVuori N160
27	Ramshot Zip	77	Alliant Reloder 10X	127	Hodgdon H4831 & H4831SC
28	Hodgdon HP-38	78	VihtaVuori N130	128	Hodgdon SUPERFORMANCE
29	Winchester 231	79	IMR, Co IMR 3031	129	IMR, Co IMR 4955
30	Alliant 20/28	80	VihtaVuori N133	130	Winchester Supreme 780
31	Alliant Unique	81	Hodgdon BENCHMARK	131	NORMA MRP
32	Hodgdon UNIVERSAL	82	Hodgdon H335	132	Alliant Reloder 22
33	IMR, Co IMR UNEQUAL	83	Ramshot X-Terminator	133	VihtaVuori N560
34	Alliant Power Pistol	84	Accurate Arms 2230	134	VihtaVuori N165
35	VihtaVuori N330	85	Accurate Arms 2460s	135	IMR, Co IMR 7828
36	Alliant Herco	86	IMR, Co IMR 8208 XBR	136	Alliant Reloder 25
37	Winchester WSF	87	Ramshot TAC	137	VihtaVuori N170
38	VihtaVuori N340	88	Hodgdon H4895	138	Accurate Arms Magpro
39	Hodgdon Hi-Skor 800-X	89	VihtaVuori N530	139	IMR, Co IMR 7977
40	Ramshot True Blue	90	IMR, Co IMR 4895	140	Hodgdon H1000
41	Accurate Arms No. 5	91	VihtaVuori N135	141	Ramshot Magnum
42	Hodgdon HS-6	92	Alliant Reloder 12	142	Hodgdon RETUMBO
43	Winchester AutoComp	93	Accurate Arms 2495BR	143	VihtaVuori N570
44	Hodgdon CFE Pistol	94	IMR, Co IMR 4166	144	Accurate Arms 8700
45	Ramshot Silhouette	95	IMR, Co IMR 4064	145	VihtaVuori 24N41
46	VihtaVuori 3N37	96	NORMA 202	146	Hodgdon H50BMG
47	VihtaVuori N350	97	Accurate Arms 4064	147	Hodgdon US869
48	VihtaVuori 3N38	98	Accurate Arms 2520	148	VihtaVuori 20N29
49	IMR, Co IMR BLUE	99	Alliant Reloder 15		
50	Winchester 572	100	VihtaVuori N140		

Note, powders highlighted in yellow have been used for decades of AVGR operations, those highlighted in green were specifically selected for these studies.

For each powder type, a 3/16" diameter, aluminum sphere was shot into an aluminum foil witness sheet (see figure 7) using different powder loads. High-speed video was used to observe the impact event and gain insight into the size, number and distribution of secondary impactors. In general, these particulates could be grouped into three size categories: (1) Large, 100's of microns in their longest dimension, and seemingly comprised of unburnt powder grains; (2) Medium, 10's of microns, and consisting of partially burnt grains; and (3) Small, less than 10 µm, and not sizable enough to confidently determine composition. The "small" particulates may have been soot and/or other combustion products but were deemed to have insufficient mass to be of concern and, hence, were ignored for this study. Table 3 show the performance results for these tests.

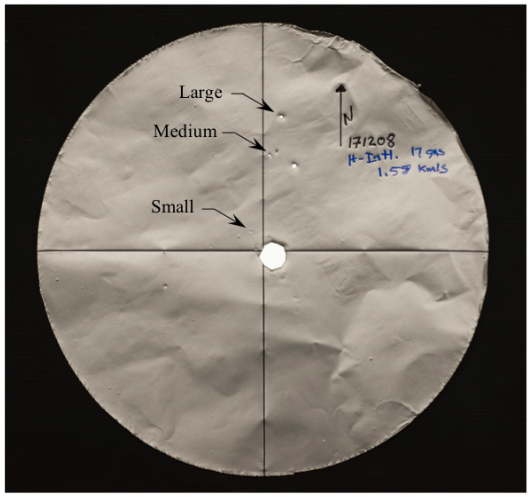

Figure 7: Foil witness sheet with large, medium and small secondary impacts.

Table 3: Powder Gun Test Results using the Standard .300 Weatherby Casing

Shot #	Powder Type	Mass (grains)	Velocity (km/s)	# of Secondary Impactors	
				Large	Medium
171223	Unique	10	1.00	4	8
171225	Unique	20	1.51	2	6
171226	Unique	25	1.71	2	1
171227	Unique	27	1.79	1	4
150601	Unique	30	1.92	1	1
171012	H-Universal	10	1.07	2	5
171208	H-Universal	17	1.58	2	4
171207	H-Universal	20	1.62	1	1
171013	H-International	10	1.14	4	2
171228	H-International	19	1.65	2	2
171224	H-International	20	1.71	0	1
171015	H-Clays	9	1.22	3	2
171014	H-Clays	10	1.26	1	1
171209	H-Clays	10	1.25	0	1
171206	H-Clays	14	1.50	1	0

Although the small sample size doesn't provide an abundance of statistical certainty, some useful, general tendencies can be gleaned from these test results. For instance, faster burning powders produce a higher velocity for a given powder charge. Also, higher speed conditions yield cleaner results for all of the powders tested. Which suggests, the greater the powder charge, the greater the combustion efficiency (more complete consumption of the combustible constituents). In addition, it was found that Hodgdon "Universal" provides similar performance to, yet is cleaner burning than, Alliant "Unique" for this particular application. Taking this a step further, if we define a "clean" shot as one that has no more than 1 large and 1 medium secondary impact, the results suggest the fastest burning powder tested, Hodgdon Clays, provides the slowest "clean" condition, approximately 1.25 km/s. Likewise, the minimum "clean" velocity for Universal, International and Unique, appear to be approximately 1.6, 1.7 and 1.9 km/s respectively.

Additional tests are needed (and shall be conducted when time and resources permit) to statistically establish a more precise "clean" minimum threshold for each of the powders. Yet, it is clear Hodgdon Clays and Universal are cleaner alternatives to Alliant's Unique when used to operate the AVGR .30 cal. powder gun. Lastly, there are a handful of still faster burning powders that could potentially provide even slower "clean" conditions using the standard casing in the AVGR powder gun. Plans for examining the performance of these powders are still in their infancy and, undoubtedly, they too will have lower "clean" limits. Furthermore, if the "clean" criterion of one large and one medium secondary impactor is deemed "not clean enough" for a specific experiment, then another approach needs to be developed (please see parts B and C).

B. Custom (Reduced Volume) Casing

In a parallel effort to develop "clean" test conditions for velocities at or below 1.9 km/s, a custom casing with only 25% of the internal volume of the standard .300 Weatherby casing was designed and fabricated. Figures 6a and 6b show sectional views of the two casings. As with the previous series of experiments, all three Hodgdon powders (Universal, International and Clays)

were used to shoot 3/16" diameter, aluminum spheres into aluminum foil witness sheets. The results of these test are listed in Table 4.

Table 4: Powder Gun Test Results using the Custom Casing

Shot #	Powder Type	Mass (grains)	Velocity (km/s)	# of Secondary Impactors	
				Large	Medium
171203	H-Universal	3	0.48	7	20
171205	H-International	3	0.62	8	10
171201	H-Clays	3	0.88	5	25
171115	H-Universal	5	0.89	20	17
171204	H-International	5	1.14	10	14
171202	H-Clays	5	1.42	3	16
171114	H-Clays	10	2.00	0	4

As expected, the smaller casing volume improved the combustion efficiency which increased the velocity for a given powder load. For example, 10 grains of Hodgdon Clays in the standard casing yielded an impact velocity of 1.25 km/sec (see Table 3). Whereas the same load in the custom casing yielded 2.0 km/sec (see Table 4). Disappointingly, however, the custom casing produced significantly more secondary impacts for a given velocity than the standard casing. In fact, none of the custom casing shot conditions yielded "clean" (no more than 1 large and 1 medium secondary impact) results. In addition, a 5-grain load was found to be a safe upper limit or maximum powder charge for the custom casing. Using a 10-grain load over-pressurized and deformed the casing. In conclusion, it would appear that reducing the casing volume is not an effective means to provide clean test conditions for the AVGR .30 cal. powder gun.

C. Light-Gas Gun Parametric Variations

A third approach that was studied as a means to provide "clean" low speed test conditions involved parametric adjustments to the AVGR .30 cal. two-stage, light-gas gun. This gun is inherently cleaner than its powder gun counterpart by virtue of the fact it's propellant medium (usually compressed hydrogen) is devoid of gun powder combustion products. However, sub-micron size soot particles do get entrained in the trailing gas stream and tend to arrive at the target 10's of milliseconds after the impactor. Using the gun gases suppression valve readily nullifies this issue and keeps targets clean. As such, the main challenge with this approach was finding a means to reduce the minimum speed to fall within the range of interest. In its decades-long traditional mode of operation (using hydrogen as the propellant medium and Hodgdon H-4895 smokeless powder as the first stage driver), the AVGR light-gas gun has a lower velocity limit of approximately 2.5 to 3 km/sec over its standard range of launch masses. In an attempt to lower this, a slower burning powder, IMR-4831, was substituted for the traditional H-4895 (once again, see table 2 for relative burning rate comparisons). In addition, helium or argon was substituted for hydrogen. Ordinarily, using these gases in place of hydrogen would tend to increase gun barrel erosion rates which, in turn, would reduce barrel longevity [2]. However, for these slow speed conditions, there was no discernable change in gun barrel erosion rate. Table 5 shows the results of these comparative studies.

Table 5: Light-Gas Gun Test Results

Shot #	Gun Powder Type	Gun Powder Mass (grams)	Pump Tube Gas	Pump Tube Press. (psi)	Velocity (km/s)
171210	H-4895	50	Hydrogen	40	2.63
091018	H-4895	40	Hydrogen	40	2.48
171211	IMR-4831	50	Hydrogen	40	1.92
171218	IMR-4831	40	Hydrogen	40	1.83
171221	IMR-4831	50	Helium	40	1.50
171213	IMR-4831	40	Helium	40	1.45
171222	IMR-4831	50	Argon	40	0.84
171216	IMR-4831	40	Argon	40	0.81

Once again, for each test, a 3/16" diameter aluminum sphere was shot into a foil witness sheet to verify the gun was operating cleanly (which it did for every test). In general, it was found that switching from H-4895 to the slower burning IMR-4831 yielded a 27% reduction in velocity. Likewise, substituting helium for hydrogen reduced the velocity by 21% and substituting argon for hydrogen reduced the velocity by 56% (see figure 8).

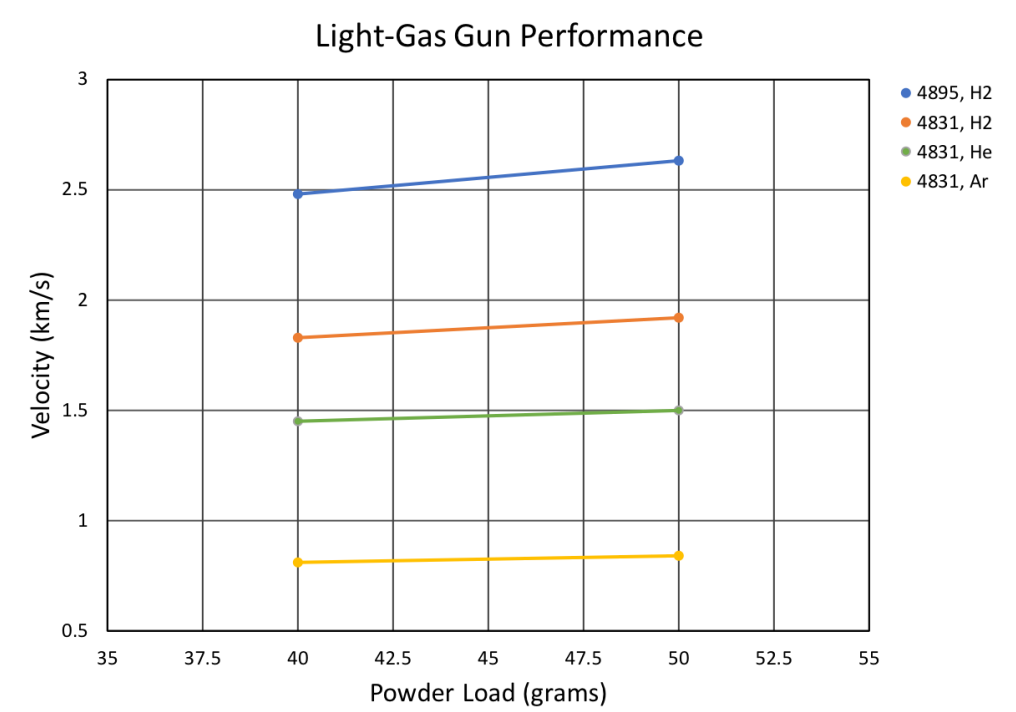

Figure 8: Velocity vs Gun Powder Load plot for various powder types and pump tube gases.

It should be noted these values are very approximate due to the small sample size (only one test at each condition and for only two powder loads). None-the-less, it is quite clear that a judicious selection of gun powder type and pump tube gas provides a very effective means to

reduce the minimum impact velocity of the AVGR .30 cal. two-stage, light-gas gun to less than 1.0 km/s. Furthermore, when operated in conjunction with the gun gases suppression valve, the test conditions are extremely clean and devoid of secondary impacts or soot deposition.

In conclusion, it was demonstrated that switching from Alliant Unique smokeless powder to Hodgdon Universal and Clays provides an effective means to lower the projectile velocity for the "clean" operating threshold for the AVGR .30 cal. powder gun, using the standard .300 Weatherby casing, from 1.9 to 1.25 km/s. Using a custom (reduced volume) casing increases the velocity for a given powder charge but also increases the number of secondary impacts. In addition, it was shown that very clean conditions down to 1.0 km/s are possible using the AVGR .30 cal. light-gas gun by selecting an appropriate combination of powder type (H-4895 or IMR-4831) and higher molecular weight pump tube gas (helium or argon). That said, for experiments that are insensitive to minor secondary impacts, the AVGR .30 cal. powder gun is the gun of choice in that it is much more economical gun to operate.

IV. SOME "COOL" EXPERIMENTS

In fall of 2016, a series of AVGR test entries began in support of two potential NASA missions. The first being an exploratory journey to Saturn's icy moon Enceladus [9] and, the second, an investigative sojourn to the asteroid 16-Psyche [5]. During the Cassini mission, geysers of ice particulates were observed in the southern polar region of Enceladus (see figure 9, from Ref. 9). The origin of these particles is believed to be a salty, liquid ocean beneath the moon's frozen crust. It is hypothesized that hydrothermal activity periodically forces water up through a complex system of fissures that were observed in great detail by the Cassini spacecraft. As the water is expelled into cold confines of space, some 900 million miles from the warmth of the sun, it instantly freezes into tiny ice particulates. The goal of this mission is to send a spacecraft to Enceladus, fly through the ice plumes and collect material, analyze it for signs of life [7] and, perhaps, answer the profound question, "Are we alone in the Universe?" Toward this end, super cooled (to temperatures less than -150° C) ice targets were subjected to hypervelocity impact to generate ejecta plumes of small ice particulates (see figure 10). The particle velocity and size distribution in certain regions of the ejecta plume are believed to be similar to what a spacecraft might encounter whilst orbiting Enceladus. Thus, providing a useful means to test the effectiveness of candidate collector designs.

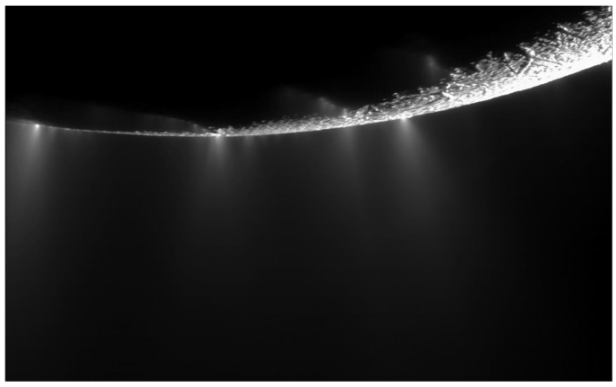

(a) Cassini image of Enceladus ice geyser plumes.

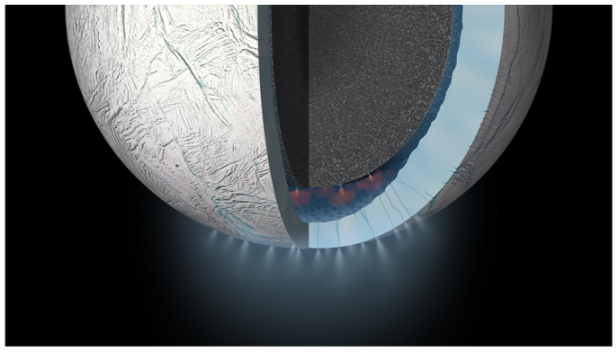

(b) Artist's concept of Enceladus interior features.

Figure 9: Saturn's icy moon, Enceladus. Cassini imagery plus artists concept of possible interior features.

The other NASA mission, now selected and in development, is an investigatory voyage to 16-Psyche, a massive (greater than 200 km in diameter) metallic asteroid that is believed to be the exposed core of an ancient protoplanet that was cataclysmically destroyed billions of years ago. For this mission, a spacecraft will be sent to 16-Psyche to establish orbit and make a variety of scientific measurements and observations to map out the geo-morphology, magnetic field and gravity characteristics of this metallic world. The mission will also provide a unique opportunity for scientists to "take a look" at a planet's core. AVGR testing in support of this mission involved shooting into a variety of metallic meteorite fragments and asteroid analogs, both at ambient and at super cool temperatures, to gain insight as to how target temperature affects crater morphology for hypervelocity impact. This information is now being used by mission scientists to develop a reasonable expectation of the type of crater landscape that will likely be encountered when the spacecraft arrives at 16-Psyche in 2026.

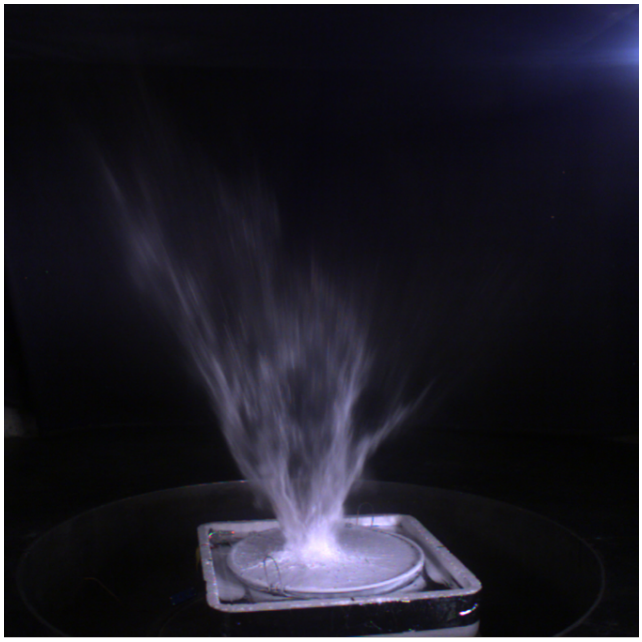

Figure 10: Impact generated ice particulate ejecta plume.

A. Active Cooling

For many of the Enceladus mission experiments, it was necessary to have the ice targets and collector array(s) chilled to temperatures below -150° C during the impact and particle capture events. Toward this end, targets and collectors were initially cooled to approximately -186° C, by immersion in a bath of LN_2 (see figure 11) with subsequent extraction from the bath and installation in the impact chamber as the "final step" before securing and evacuating the chamber. For most of these tests, the AVGR vacuum pumping system was sufficiently robust to achieve desired vacuum levels before the collector and ice target temperatures rose above the -150° C threshold. However, during the brief exposure to the atmosphere, a frost layer typically formed on the collector surfaces. In fact, ambient moisture would begin condensing and freezing immediately after the collector was removed from the LN_2 bath. Understandably, there was concern that such a frost layer might affect results. That is, the particle motion within a collector and, ultimately, how much material successfully enters the collection chamber.

Figure 11: Collector/Target immersion in LN_2 bath for super cooling.

To mitigate the frost layer and assuage associated concerns, an active cooling system was designed and implemented to allow cooling the collectors after installation in the chamber and while at vacuum, wherein there is presumably insufficient moisture to cause appreciable frost accumulation. The resulting active cooling system (see figure 12 schematic) consists of: a pressurized, liquid nitrogen dewar (Taylor-Wharton XL65, 240-liter); a robust, stainless-steel feedthrough flange; a pair of bulkhead fittings suitable for cryogenic service (courtesy of MDC Vacuum Products); and insulated, ¼" tubing (Swagelok) and flex hoses (Cryofab).

Part	Item Description	Qty.
1	Flex hose, Cryofab CFUL-050-0214-A-2, 1200 psi MAWP, ¼" FNPT & CGA295 ends	1
2	Flex hose, Cryofab CFUL-050-1414-A-6, 1200 psi MAWP, ¼" FNPT ends	2
3	Bulkhead connector, MDC UHV611041, ¼" Swagelok connectors, 316-SS	2
4	Tubing and fittings, ¼" 0.035" wall SS, Swagelok unions, elbows and connectors	
5	Tubing and fittings, ½" 0.049" wall SS, Swagelok unions and elbows	
6	Flange, 304-SS Class 150 ASME B16.5, 11" dia. w/9.5" BC and two 1" thru holes	1

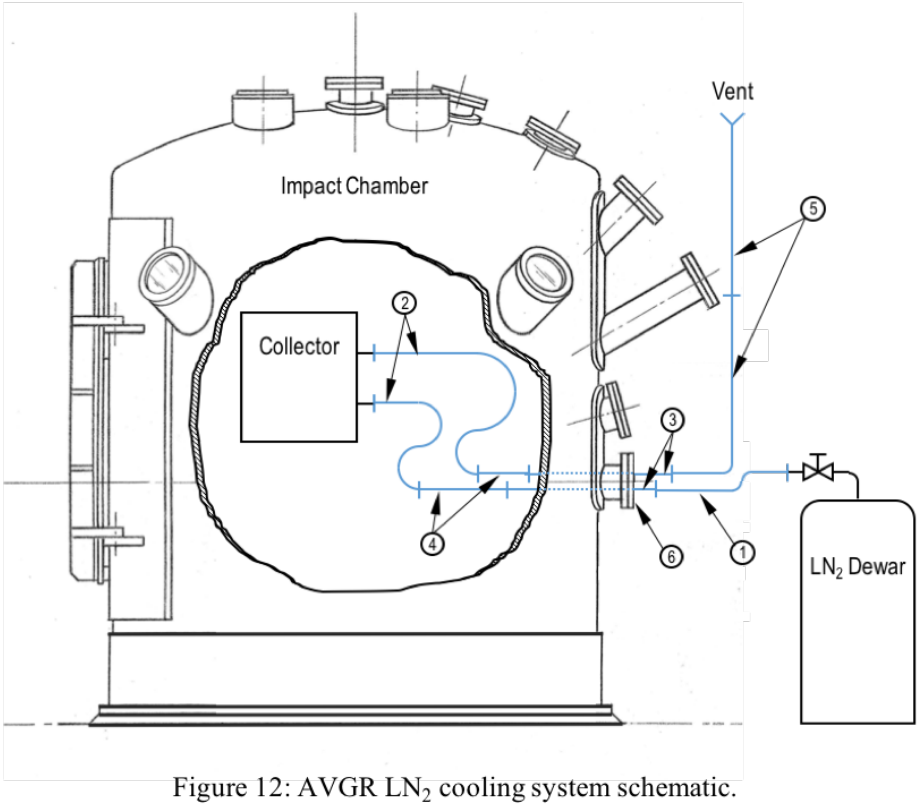

Figure 12: AVGR LN_2 cooling system schematic.

Straightforward and practical, the system allows flowing LN_2 into the impact chamber, through the collector cooling coils, back out of the chamber and, ultimately, venting directly to the atmosphere. To verify moisture levels are sufficiently low so that cooling can commence, a temperature & humidity sensor (Vaisala HMT330) has been added to the repertoire of chamber instrumentation. This device, combined with a pre-existing, multichannel, k-type, thermocouple system (Omega RDXL6SL) enables recording the time history of collector/target temperature(s), peripheral equipment and materials temperatures, and chamber temperature and humidity levels during an experiment.

In addition, in order to satisfy NASA Ames pressure systems safety regulations, a large pressure relief valve was designed, fabricated and installed on the impact chamber so as to eliminate the possibility of over pressure in the event of a large LN_2 leak within the impact chamber. This relief valve (see figure 13) was constructed from 4" class 150, aluminum pipe fittings. Simple, yet effective, it uses the weight of a horizontal lift plate (aluminum flange blank) to maintain a seal while the chamber is at or below atmospheric pressure. A chamber pressure of 0.5psi above ambient is sufficient to create a pressure force that exceeds the weight of the lift plate, thus, causing it to lift and vent. Although originally intended for exclusive use with the LN_2 system, this device is now a permanent installation.

Figure 13: Vacuum/Impact Chamber Relief Valve.

The active cooling system proved to be quite effective at maintaining collector temperatures at or below -150° C for the Enceladus test series. Beginning the cool down process while the chamber was at vacuum definitely reduced the amount of frost build up and what little frost did condense, typically occurred at the flex hose fittings and coils rather than on the data critical collector surfaces (see figure 14). Lastly, target geometry and whether it uses externally wrapped cooling coils or internal cooling passageways can profoundly affect the cooling rate, temp distribution (at depth vs surface) and minimal achievable temperature. Hence, careful consideration must be made when designing an actively cooled target.

(a) Active cooling initiated at atmospheric pressure

(b) Active cooling initiated at vacuum (0.1 atm)

Figure 14: Enceladus collector tests utilizing active cooling. Notice how initiating cooling while under vacuum vs. atmospheric pressure dramatically reduces the amount of frost build up.

B. Passive Cooling

As mentioned previously, some of the targets that were impacted in the Psyche mission experiments were metallic meteorite samples for which the investigators requested target temperatures at impact to be at or below -140° C. Specifically, the targets were small cubes measuring roughly 1.5” x 1.5” x 1.5” (38 x 38 x 38 mm) that were machined from fragments of Gibeon, Santiago Papasqueiro and Coahuila meteors. Given this diminutive size and cubic shape, there was no practical way to wrap the targets with cooling coils. Likewise, drilling them to create internal passageways would have compromised the structural integrity of the specimens, making them prone to complete disruption upon impact plus it would have minimized the number of surfaces suitable for impact. Thus, there was no apparent, active cooling option. In addition, given their small thermal masses, these targets were prone to warming up well above -140° C during the time that elapsed between removal from the LN_2 bath and impact.

To remedy this challenging situation, targets were affixed atop a 4” x 4” x 2” (102 x 102 x 51 mm) copper block which would serve as a sizable thermal mass (see figure 15). The whole assembly (initially at ambient conditions in the laboratory) was subsequently immersed in LN_2 until both the block and target reached thermal equilibrium (roughly -186° C). Then, the assembly was quickly transferred to an insulated target holder, positioned in the impact chamber, thermocouple leads connected, and chamber secured. The resultant target temperature at impact remained quite low (between -150° C and -160° C, well below the -140° C acceptable maximum), by virtue of conductive heat transfer to the copper cold sink. It should be mentioned that a thin frost layer did indeed form on the target surfaces. However, the investigators deemed this acceptable given the size and mass of the impactors, the velocity of the impacts, plus they believe it’s likely there is a thin layer of pulverized material on the surface of 16-Psyche for which the thin frost layer might actually be a suitable analog.

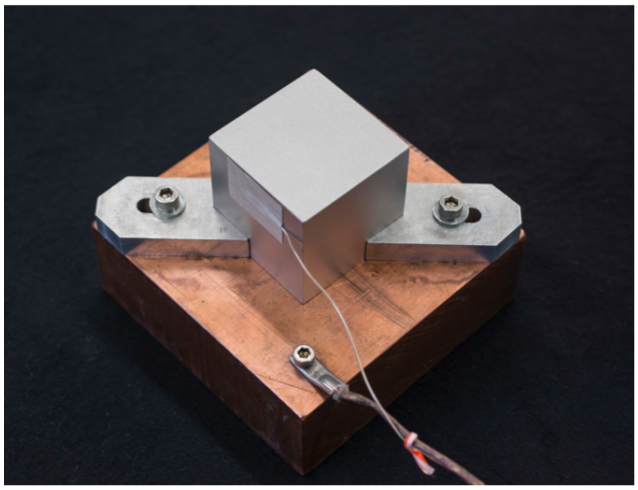

Figure 15: Psyche Mission test article: Meteorite sample affixed to a copper, thermal mass. Both items equipped with a type-k thermocouple.

One additional important lesson learned warrants mentioning. Between tests the copper block needed to be warmed back up to room temperature before affixing another target and starting the chilling process anew. Any attempt at using a cold block resulted in a thin, insulative layer of frost forming between the target and block surface. This was found to significantly reduced the heat transfer between the copper cold sink and the target, with the result being a target temperature at or above the -140° C acceptable maximum at the time of impact. There simply was no way to remove the frost and install the target without this layer reforming.

C. Imaging System Enhancements

During the Cassini Mission flybys, it was observed that the population density of Enceladus plume ice particulates is heavily concentrated in the 10’s of microns size range. In order to capture

particles of this size, many of the proposed collector designs were/are conical in shape with a central spike to help direct the particulates through a small annular ring at the base of the spike/collector cone and into a collection chamber. The primary differences between the various designs that were tested in the AVGR were with the cone & spike angles and the size of the annular passage ways. Several test entries were conducted to evaluate how well candidate collectors capture particulates [9] and how well organic molecules survive the capturing process [7]. Figure 14 (from Ref. 9) shows a generic, 2-D, segmented, collector model that was used for such purposes.

(a) Standard camera arrangement for Enceladus collector testing

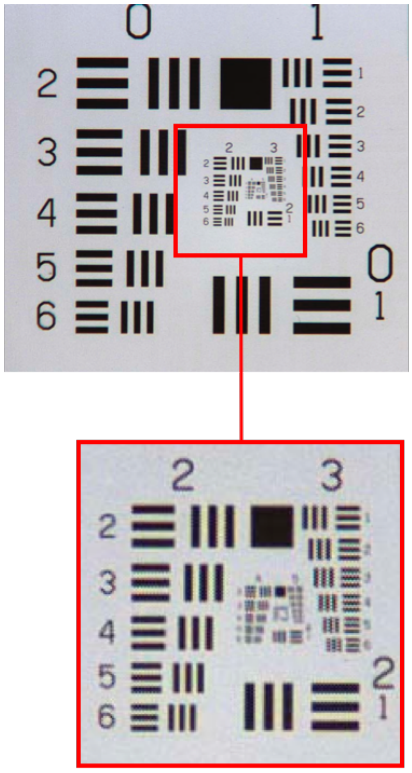

(b) Still frame image of a 1951 USAF Resolution chart

Width of 1 line in micrometers in USAF Resolving Power Test Target 1951									I51
Group Number									
Element	-2	-1	0	1	2	3	4	5	6
1	2000.00	1000.00	500.00	250.00	125.00	62.50	31.25	15.63	7.81
2	1781.80	890.90	445.45	222.72	111.36	55.68	27.84	13.92	6.96
3	1587.40	793.70	396.85	198.43	99.21	49.61	24.80	12.40	6.20
4	1414.21	707.11	353.55	176.78	88.39	44.19	22.10	11.05	5.52
5	1259.92	629.96	314.98	157.49	78.75	39.37	19.69	9.84	4.92
6	1122.46	561.23	280.62	140.31	70.15	35.08	17.54	8.77	4.38

(c) Resolving power table for 1951 USAF Resolution chart

Figure 16: Imaging system upgrades for Enceladus testing: V2512 monochrome camera, 400mm lens, 2X multiplier, extension bellows, 1280 x 720 resolution, 28,000fps, 280ns exposure yields 40µm resolving power.

In addition, high-speed video imagery was requested by the mission team so as to verify computational models that predict particulate trajectories within the collector and to actually "see"

what ends up in the collection chamber. Photographically resolving particles on the order of 50 μm traveling at 1 – 2 km/s was not something that had been previously done in the AVGR. Many iterations combining different lenses, focal length multipliers, extension tubes, lighting configurations, frame rates, exposure times and resolution levels were explored until, finally, a suitable combination was found. In the end, a monochrome version of the Phantom V2512 camera (courtesy of Vision Research) utilizing a frame rate of 28,000 fps, an exposure time of 285 ns and a resolution of 1280 x 720, paired with a 400 mm lens, proved a successful combination. Figure 16 shows the system set-up, and a still frame image of the classic USAF 1951 resolution target (demonstrating satisfactory resolving power down to ≈ 40 μm).

One facet of this enhanced imaging technique that proved particularly challenging was concentrating ample light upon the subject area. Light emitting diodes (LED's) proved to have insufficient intensity/radiant energy and yielded inconsistent contrast due to their non-continuous (pulsating) operation. A laser light source may have been a workable option, however, for this entry there wasn't sufficient time or funding to develop and implement such a system, its operating procedures & safety protocols, or to ensure the camera sensor wasn't going to incur any damage. Eventually, six PAR-64, 1000 W, tight-spot, lamps in close proximity to a diffusive sheet/screen and directed toward the collection chamber proved sufficient to produce a back-lit, shadowgraph-like video sequence. Figure 17 shows the lighting arrangement plus collection chamber images, using the aforementioned set-up, before and during a particle capture.

(a) Typical lighting & diffuser screen arrangement to illuminate collector and collection chamber.

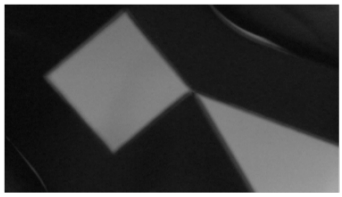

(b) Collection chamber image prior to particulate arrival

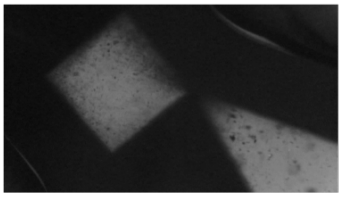

(c) Collection chamber image during particulate capture

Figure 17: Enceladus collector test set-up (utilizing active cooling and imaging system enhancements) plus excerpt images from a typical particle capture sequence.

Interestingly, although the enhanced imaging system set-up proved to be quite successful in capturing the desired imagery, the radiant intensity was so large that it caused most of the captured particulates to sublime shortly after the capture event. This, in turn, left an insufficient quantity of material to collect for organic survivability testing. As a result, for this particular situation, it was found that one can either observe the particles or collect material for subsequent analysis but not both for the same test. Furthermore, operating the lighting system for too long can melt or burn the diffusive sheet and/or the supporting wooden framework and it accelerates the warm-up rate for the collector and ice target.

V. SUMMARY AND CONCLUSIONS

Recent upgrades to the performance capabilities of the NASA Ames Vertical Gun Range (AVGR) were presented. Among these was the successful implementation of a fast-acting, gun-gases suppression valve. This portable device can be used at any of the gun orientation ports and was shown to effectively minimize target contamination and perturbations to both the target and ejecta for light-gas gun testing and, to a lesser extent, powder gun testing. For velocities below 1.9 km/s (traditionally within the realm of powder gun operations and well below the traditional lower limit for light-gas gun operations), the suppression valve alone was insufficient to eliminate secondary impacts from unburnt and partially burnt gun power grains.

To mitigate this effect, gun powders with different burning rates were examined. Using the fastest burning powder tested, Hodgdon Clays, successfully lowered the "clean" threshold from 1.9 to 1.25 km/s. In addition, a custom casing with only 25% of the internal volume of the standard bullet casing used for powder gun operations was tested. Although, the velocity for a given powder charge increased dramatically so did the number of secondary impacts. Hence, this approach was deemed ineffective.

As an alternative means to provide clean, low speed test conditions, parametric variations for light-gas gun operations were also examined. Specifically, substituting helium or argon in place of hydrogen as the pump tube gas, plus using the slower burning IMR-4831 gun powder in place of the traditional H-4895, successfully reduced the lower operating limit for the AVGR light-gas gun from 3 to less than 1 km/s. Given that light-gas gun testing is more expensive and time consuming than powder gun testing, this option should be used only when deemed absolutely necessary.

In order to enable the AVGR to provide critical testing in support of proposed NASA missions to Enceladus and 16-Psyche, a liquid nitrogen-based system and methodology for actively and passively cooling targets and/or other impact chamber situated equipment, plus a target temperature & chamber environmental conditions monitoring system were developed and put into service. In addition, a robust pressure relief device to prevent impact chamber over pressurization in the event of a large LN_2 leak was design and installed. As a result, the AVGR can now accommodate super-cooled targets and/or other impact chamber situated equipment and provide continuous monitoring of target and chamber conditions. Moreover, the high-speed video imaging system can now be configured to allow observing particles as small as 50 μm traveling at 1 – 2 km/s.

All together, these recent upgrades have markedly improved and expanded the performance capabilities of the Ames Vertical Gun Range, especially in the low speed (<2 km/s) portion of the operational envelope and have provided for the accommodation of chilled targets & equipment. Furthermore, these recent experiments have identified promising avenues of exploration to

develop and expand these capabilities even further. Lastly, NASA does not officially endorse any of the products or manufacturers mentioned in this paper. Rather, these details are provided for illustrative purposes only.

ACKNOWLEDGEMENTS

The authors would like acknowledge and thank: Don Bowling and Adam Parrish, members of the AVGR operations team, for their tireless help and support in generating the experimental data for this paper; Dr. David Bogdanoff for sharing his wealth of experience and providing valuable suggestions and guidance for the parametric studies that were explored; and Dr. Michael Wilder for his editorial expertise and guidance in navigating the often frustrating terrain (i.e. Power Point, Word, etc.) of technical paper crafting. Lastly, the authors would also like to thank our frequent visiting researchers whose work inspired this effort. This includes: David Willson (KISS Institute for Practical Robotics), Dr. Daniel Durda (SwRI), Dr. Simone Marchi (SwRI), Dr. Steven Jones (JPL) and Dr. Peter Schultz (Brown University).

REFERENCES

1. Bogdanoff, D. W., "New Higher-Order Godunov Code for Modelling Performance of Two-Stage Light Gas Guns," NASA TM 110363, September, 1995.
2. Bogdanoff, D. W., "CFD Modelling of Bore Erosion in Two-Stage Light Gas Guns, NASA TM-1998-112236, August, 1998.
3. Canning, T. N.; Seiff, A. and James, C. S., "Ballistic Range Technology," AGARDograph 138, published by the North Atlantic Treaty Organization, Advisory Group for Aerospace Research and Development (AGARD), August, 1970, p. 158 - 166.
4. Cornelison, C. J., "Status Report for The Hypervelocity Free-Flight Aerodynamic Facility," 48th Aeroballistic Range Association Meeting, November 1997.
5. Durda, D. D., Marchi, S., Grosh, D. J., Chocron, S., Walker, J. D., Housen, K. R., "Impact Experiments with Iron-Nickel Targets: Momentum Enhancement and Crater Morphology," 48th Lunar and Planetary Science Conference, March 2017.
6. Hodgdon Powder Company, www.hodgdon.com, "Relative Burn Rates, From Fastest to Slowest," November 2016.
7. McKay, C.P., Willson, D., Bonaccorsi, R., Thomson, S., Koehne, J., "Effect of High Velocity Collection on Trypsin functionality for Life Detection," 2017 Science Innovation Fund, Preliminary Findings Report, December 2017
8. Wilder, M. C., Bogdanoff, D. W., and Cornelison, C. J., "Hypersonic Testing Capabilities at the NASA Ames Ballistic Ranges," AIAA 2015-1339, 53rd AIAA Aerospace Sciences Meeting, January 2015.
9. Willson, D., Gold, R., Bonaccorsi, R., Slone, D., Mathias, D., Thomson, S., Koehne, J., and McKay, C.P., "Catching Life in the Icy Plumes of Europa & Enceladus," Astrobiology Science Conference, April 2017
10. Terrazas-Salinas, I. "Test Planning Guide for the NASA Ames Research Center Arc Jet Complex and Range Complex," A029-9701-XM3 Rev. C, April 2009, p. 47 - 55.
11. Vision Research Inc., www.phantomhighspeed.com, "Datasheet for Phantom V10, V12.1 and V2512 Cameras," January 2017.